1958, Beard 1962, Whitmore 1971), which suggests that the de Villiers (1982) figure is an overestimate. Sophisticated models of interception loss, such as those by Rutter *et al* (1971) and Gash (1979) allow for evaporation from wetted surfaces during and after the storm. For the short-duration high-intensity storms characteristic of semi-arid savannas, however, it is pragmatic to ignore evaporation which occurs during the storm. Assuming that the plant has a negligible ability to absorb moisture directly through its canopy surface, interception loss per storm can then be equated to the canopy storage volume for a fully saturated canopy, this being the amount of water available for evaporation after the storm. The canopy storage volume is that quantity of water held on the wetted exterior of a plant against gravity. It is composed of a leaf storage volume and a stem storage volume, and for the purposes of this study is treated as a constant per unit area of each substrate, regardless of storm intensity, wind direction and speed.

Leaf and stem storage volumes were determined for the dominant tree and grass species at each site by measuring the increase in mass of fresh leaf and bark sample after wetting with a fine mist spray. The surface volumes for the entire plant were calculated from regressions of leaf and stem surface area against stem diameter. The values for the storage volume of tree leaves appear in Table 3.8, and the regressions in Table 4.1.

Simulation modelling revealed these estimates to result in net interception losses considerably lower than published estimates, which are in the range of 5-10% of the annual precipitation. The method of estimating canopy storage volume may have underestimated the true storage volume, or the evaporation during the storm may be higher than expected.

3.3 RUNOFF AND INFILTRATION

The precipitation which reaches the ground surface either percolates into the soil (infiltration) or runs off the soil surface (runoff), initially as overland flow and ultimately as streamflow. Infiltration and runoff are thus complementary, and will be discussed as a single phenomenon.

Runoff is of paramount importance to engineering hydrologists and soil conservationists and there is a good empirical knowledge of the factors that influence it (Morgan 1979). There is however no definitive physical description of the process of infiltration, despite much interest in the field (Philip 1969). Equations of many forms can be fitted to steady-state cumulative infiltration data (Collis-George 1977), and the choice of which to use is dependent on convenience rather than rigour. Most follow Philip (1969) in describing cumulative infiltration as the sum of two terms. The first (sorbtivity) is proportional to the square root of elapsed time, while the second is directly proportional to elapsed time. The infiltration rate thus tends to the saturated infiltration rate as time tends to infinity.

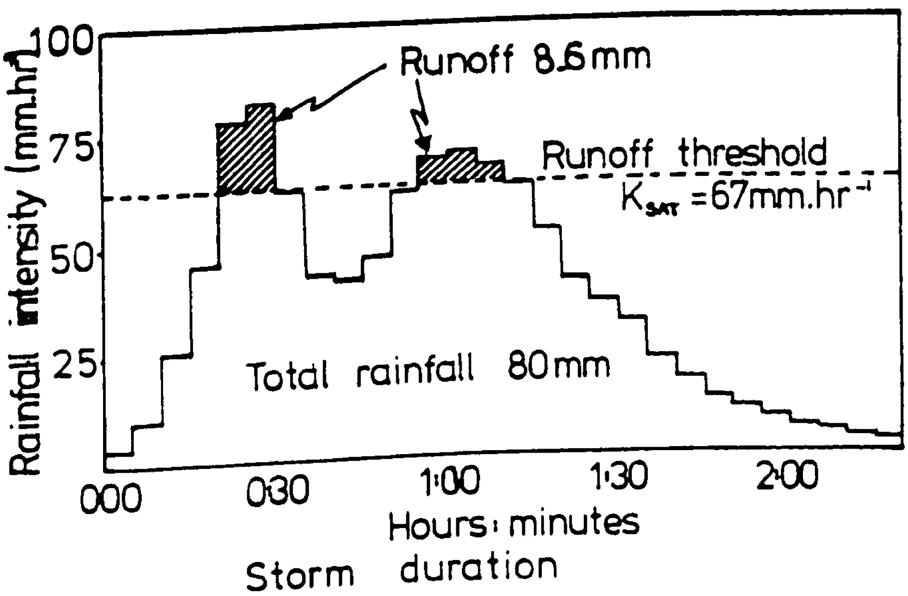

Figure 21. Calculation of infiltration rate from a storm hydrograph: a hypothetical example.

Table 3.2 Estimates of the critical infiltration rates at each site derived from runoff data and storm hydrographs.

Site	Day	Rainfall	Infiltration rate ($mm.hr^{-1}$)							
			Grassland				Woodland			
Plot		(mm)	1	2	3	4	5	6	7	8
Combretum	262	77	50					50		
	494	35	70	70				70	70	
	500	63	144			106	142	144	137	
	580	82					132	132	158	158
	634	75	96	112				89	100	106
Mopane	526	18	60	60	60	54	60	54	54	53
	630	48	151	133		151	151		133	133
	871	23	145	141	141	133	151	151		172
	883	75	175	175		152	189	175	189	175
	934	95	142	152	142	78	152	142	142	152
	956	49	84			81				
	989	39	226		226	174				
Acacia	500	57	142	152			141	132	118	
	517	24	79	79			61		79	
	526	60	152	164	164		152	152		
	527	12					73	70	73	73
	577	22	40							
	580	24	142				180	200		
	600	38	73		89		89			89
	923	30	190		190		193		193	
	932	67	61	61	61		61			
	992		112		112					

Further complexity is introduced when natural rainfall is considered rather than ponded infiltration or steady-state simulated rainfall, since natural rainfall fluctuates in intensity and energy.

Runoff was measured in each site by gauging the output of eight standard length (22 m) runoff plots with a tipping bucket flow-meter (Figure 22 on page 81). The width of the plots was 1.8 m in the Mopane site where the tree canopies were small and closely spaced, but 3.6 m in the other two sites to allow a more representative sample of the sub-canopy area.

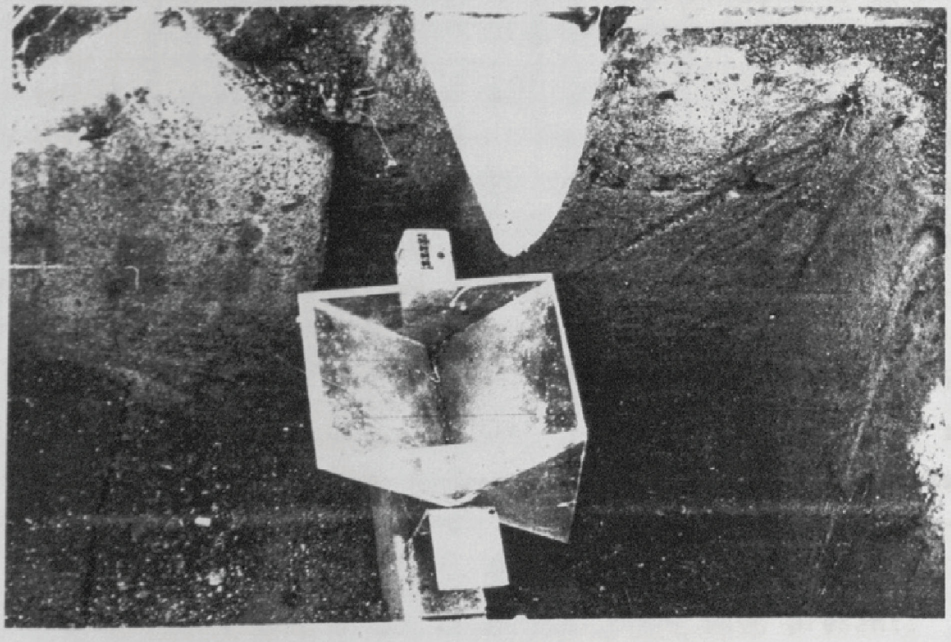

Figure 22. Runoff plot equipped with a tipping-bucket flow-meter: number of tips is recorded by a mechanical counter.

The plot walls were constructed of galvanised steel sheet (0,3 mm x 350 mm) buried to a depth of 150 mm. The plots were paired to reduce variability and construction costs, with two pairs (four plots) in the wooded and two pairs in the bush cleared area. The plots were placed so as to include tree canopies, but avoid abnormal patches such as termitaria or gullies, and were oriented perpendicular to the slope contours. They were constructed a year before bush clearing began, to allow them to stabilise and to permit a pre-clearing control runoff level to be established. The latter objective was not satisfactorily achieved due to the paucity of rainfall events during the pre-clearing season.

Total runoff is the integral of the difference between the instantaneous rate of water supply to the soil surface and the infiltration rate. The runoff per storm for each plot was expressed as a depth in millimetres by dividing the runoff volume (corrected for the gutter area) by the plot area. Storm duration, which bears little relation to the instantaneous rainfall intensity, accounted for very little of the variance in runoff yield and was ignored in further analysis. The procedure by which infiltration rate was estimated from cumulative runoff data and 5-minute rainfall rates is illustrated in Figure 21 on page 79. The assumption is that infiltration rate is constant over the period of the storm. While this is obviously incorrect (Collis-George 1977), a dynamic approach to infiltration rate would have been beyond the scope of this study.

The critical infiltration rates for storms at each site as calculated by this method are presented in Table 3.2. The variability is enormous, and is due to high spatial variability (between runoff plots) as well as high temporal variability due to variations in storm depth and intensity and ground cover conditions over the period of the study. The high variability masks any treatment effect which may have been present.

The approach of Barnes (1974) of simply plotting infiltration against storm depth suffers from a high degree of self-correlation, leading to spuriously well-fitted models. Therefore runoff was directly plotted against storm depth. The plots (Figure 23 on page 83) show a wide scatter of points. The runoff yields from the different sites cannot be directly compared since they come from storms with different characteristics. Regression lines were calculated so that they formed a maximum and minimum envelope which included most of the points. The qualitative conclusions that can be drawn from them are that the regression slope for the maximum envelope, which is inversely related to the steady-state infiltration rate, was highest on the Mopane site. The regression intercept, which is directly related to the sorbtivity factor in the Philips equation, was highest on the Mopane site and lowest on the Acacia site. Overall the Mopane site lost 2-15% of its rainfall as runoff, the Acacia site 1-7% and the Combretum site 0.5-5%.

The experimental design is pseudoreplicated so inferential statistics tests cannot be applied to the results. Runoff per treatment, as a percentage of total precipitation, is presented for each site in Figure 24 on page 84.

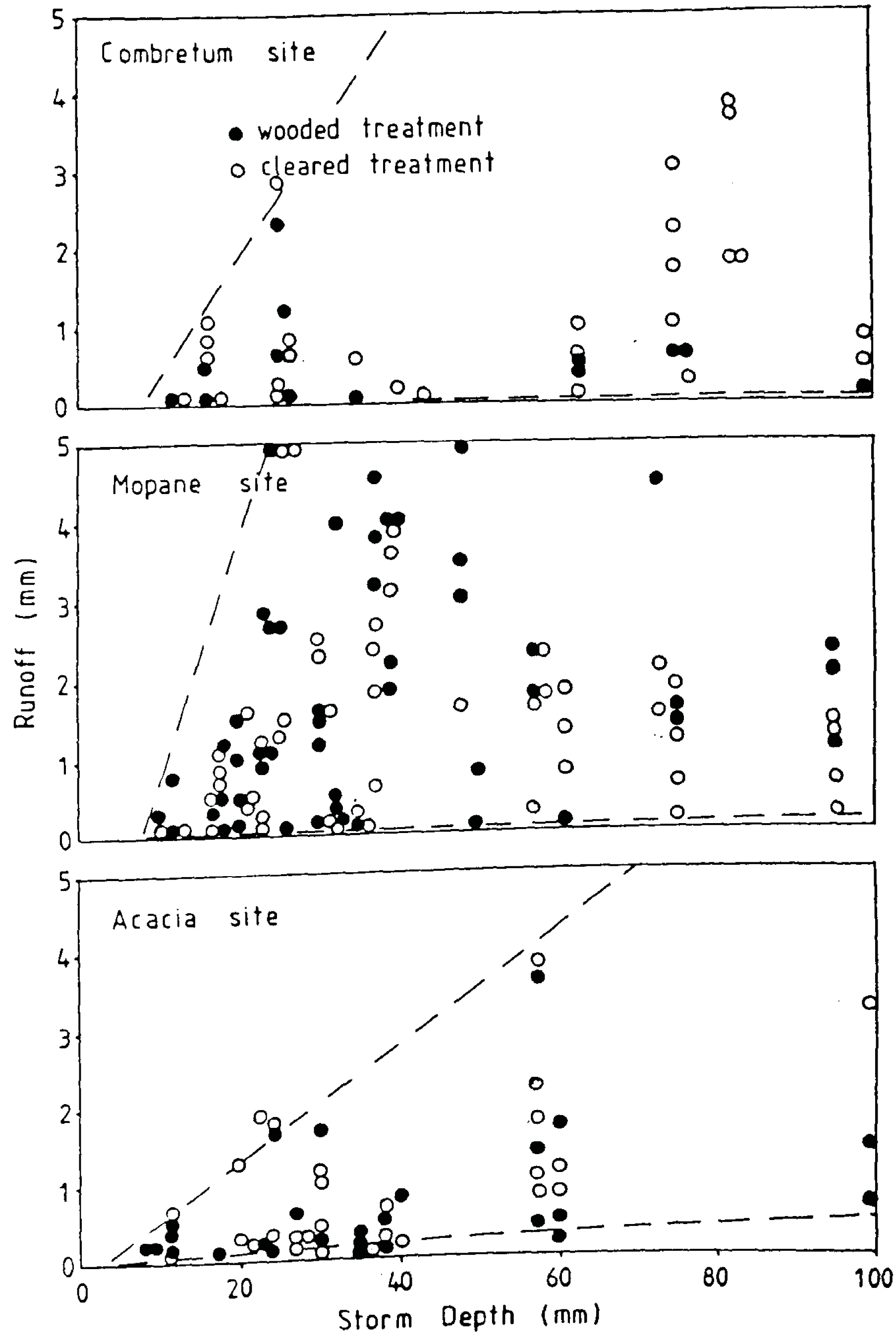

Figure 23. Plots of runoff depth versus rainfall depth: the lines represent the maximum and minimum envelopes which include most points.

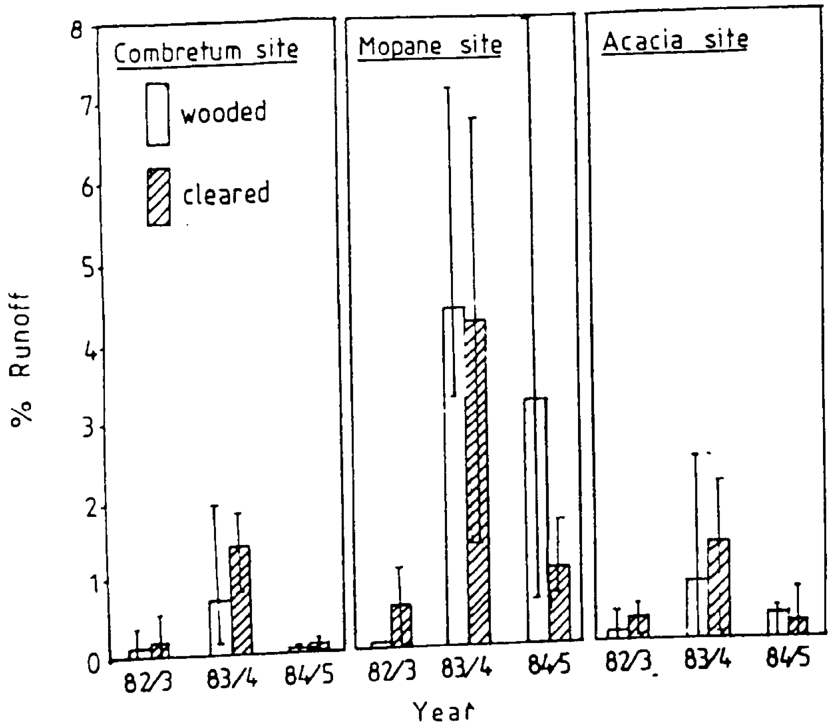

Figure 24. Percentage runoff per treatment and site: mean of four plots per treatment, bars represent the maximum and minimum range recorded. Clearing took place in the winter of 1983.

The figure shows an increase in runoff in all sites during the 1983/4 season, when the grass cover was extremely low due to the drought. The increase is greater on the cleared treatments than the control treatments at the Combretum and Acacia sites, but not at the Mopane site. There was a general trend towards lower runoff in grasslands than woodlands in the second post-clearing season, once a good grass cover was established. The variability between runoff plots is indicated by the range of values obtained. In each treatment there was at least one "rogue" plot which consistently yielded more runoff than the others, possibly due to crust formation on the surface.

The consistently greater runoff yield from the Mopane site illustrates the danger of assuming that the soil clay content continuum necessarily reflects a continuum in hydrological (or nutrient) properties. The silt content and the distribution of sand grain sizes are also important, as well as the clay mineralogy. In this case the Mopane site, a sandy loam, has a clay content (17%) intermediate between the loamy sand Combretum site (8%) and the sandy clay loam Acacia site (25%), yet the runoff yield is higher. This can be attributed to the tendency of the Mopane site soils to form both raindrop impact crusts and microfloral crusts on the soil surface, which reduce the infiltration rate. There is a higher proportion of smectitic clays at the Acacia site (inferred from the cracking in the profile) which may prevent crust formation by their self-mulching action.

3.4 SOIL MOISTURE DYNAMICS

The theoretical dynamics of soil water storage and movement have been widely studied, and a large number of empirical predictive models have been developed (Haverkamp, Vauclin, Touma, Wierenga & Vachaud 1977 and de Jong & Cameron, 1979). It is usual to divide soil moisture movement into two types, although the transition between them is continuous and broad. When the soil is at or near saturation (more than approximately 80% of the pore space is occupied by water), flow is relatively rapid and is described by Darcy's law in terms of the hydraulic head gradient (with gravitation as the major component) multiplied by the soil saturated hydraulic conductivity (K_{sat}) which is a function of pore size and tortuosity. When this "gravitational water" has drained away the soil is said to be at field capacity. When the soil is drier than this, the hydraulic gradient is dominated by the matric potential (which is a function of soil moisture content) and flow is said to be unsaturated.

The theory of flow in unsaturated porous media is based on work by Childs & Collis-George (1950) and Millington & Quirk (1961). The principal difference between saturated and unsaturated flow is that the hydraulic conductivity at soil moisture levels below saturation is strongly non-linearly related to soil moisture content (θ). Hydraulic conductivity decreases nearly exponentially with a decrease in soil moisture content, causing unsaturated flow at say 50% of field capacity to be orders of magnitude slower than saturated flow. Thus most of the movement of water in soils is due to saturated flow, especially when the soils are coarse-textured. Thus for many purposes unsaturated flow can be ignored, as it has been in previous models of savanna dynamics (Walker *et al* 1981, Walker & Noy-Meir 1982, McMurtrie & Wolf 1983). However, when there are strong hydraulic gradients in the soil and long periods between successive wetting events, unsaturated flow could be a significant component. Since these conditions frequently occur in semi-arid savannas, and small moisture fluxes could make a critical difference to coexistence models based on the differential rooting depth hypothesis, the effects of unsaturated hydraulic conductivity were included in this study.

The relationship between the hydraulic conductivity at a given soil moisture content ($K(\theta)$) and the soil moisture content is usually assumed to be unique for a given soil type (although it is probably hysteretic to varying degrees). Since it is determined by the soil matric forces, which are in turn determined by the particle size distribution, it is related to the soil moisture characteristic curve, the function that describes the dependence of soil water potential (ψ) on soil moisture content. Since both functions are difficult to determine, such a relationship would be very useful, and several attempts have been made to define it (Jackson, Reginato & van Bavel 1965, Maulem 1976). No generally accepted or universally applicable form exists for either function however, and thus the equations chosen to express (and therefore link) them are based on considerations of computational ease rather than physical theory.

The system suggested by van Genuchten (1980) has been used in this study because it is consistent, mathematically tractable and has a minimum of parameters. The problem of unsaturated flow then resolves into one of determining the parameters.

Water flow in the soil can also occur in macropores (Beven & Germann 1982). The importance of this mode of flow is largely unknown and is probably highly variable both between soil types and spatially within one soil type. Macropores are common in clays, and are probably most important there due to the low hydraulic conductivity of the bulk soil. Swelling clays present a special problem, since the vertical cracks which they develop when dry form ideal macropores, but soon close up due to the swelling of the clays once wetted; thus the $K(\theta)$ curve is not unique. The Acacia site in this study probably behaves in this manner to some degree. Once the moisture has penetrated the profile via a macropore its rate of absorption into the soil mass is limited by the rates of conventional soil water movement processes, which somewhat reduces the importance of macropore flow.

3.4.1 SOIL WATER POTENTIAL

The characteristic curves were determined on disturbed samples on a pressure plate apparatus. Two soil samples were run for each soil type and horizon at each pressure head (-30, -100, -200, -500, -1000, and -1500 kPa). The moisture content after equilibration was determined by mass loss after drying at 105 °C for 24 hours, and converted to a volumetric proportion by multiplying by the bulk density, determined by the clod immersion technique. A function of the form described by van Genuchten (1980)

$$\Theta=[1/1+(a\psi)^n]^m \quad ...3.1$$

where

$$\Theta=(\theta-\theta_{res})/(\theta_{sat}-\theta_{res}) \quad ...3.2$$

and Θ is the relative volumetric soil moisture content, θ is the volumetric soil moisture content, θ_{res} is the residual soil moisture content after prolonged air-drying, θ_{sat} is the soil moisture content at field capacity, ψ is the soil water potential (kPa) and a, m and n are constants, was fitted to the points using a statistical curve fitting routine (SAS NLIN, SAS Institute 1982) (Figure 25 on page 88). The values of θ_{sat} and θ_{res} were determined *in situ* by taking soil samples a few hours after a

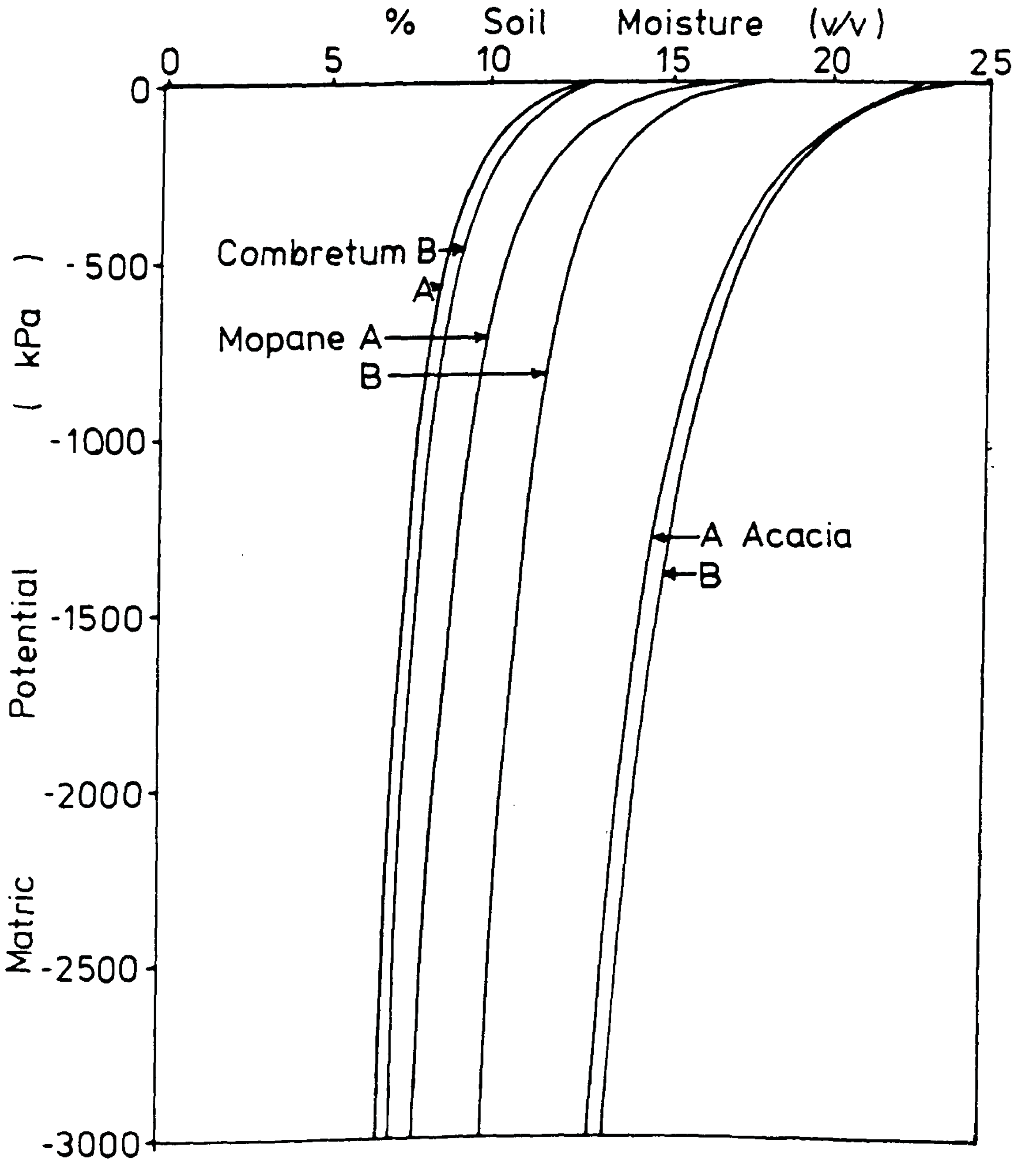

Figure 25. Soil moisture characteristic curves

large storm and after a prolonged period of drought respectively. The characteristic curve parameters for each site are given in Table 3.3.

Table 3.3 Soil characteristic curve constants.

Site	Horizon	θ_{sat}	θ_{res}	m	a
Combretum	A	0.127	0.012	0.2275	0.0231
Combretum	B	0.133	0.012	0.2306	0.0192
Mopane	A	0.165	0.017	0.2890	0.0200
Mopane	B	0.180	0.021	0.1925	0.0317
Acacia	A	0.237	0.052	0.4401	0.0048
Acacia	B	0.237	0.052	0.4011	0.0050

3.4.2 THE HYDRAULIC CONDUCTIVITY FUNCTION

The hydraulic conductivity function was derived by manipulating the characteristic curve, following van Genuchten(1980).

$$K_{rel}(\Theta)=\Theta^{\frac{1}{2}}[1-(1-\Theta^{1/m})^m]^2 \quad ...3.3$$

where

$$K_{rel}(\Theta)=K(\Theta)/K_{sat} \quad ...3.4$$

and $K_{rel}(\Theta)$ is the relative hydraulic conductivity at Θ, $K(\theta)$ is the true hydraulic conductivity and K_{sat} is the saturated hydraulic conductivity. The calculated $K_{rel}(\Theta)$ functions are illustrated in Figure 26 on page 90

The value of K_{sat} was estimated by successive approximation in order to match simulated soil moisture profiles against those measured in root-free soil columns in the field.

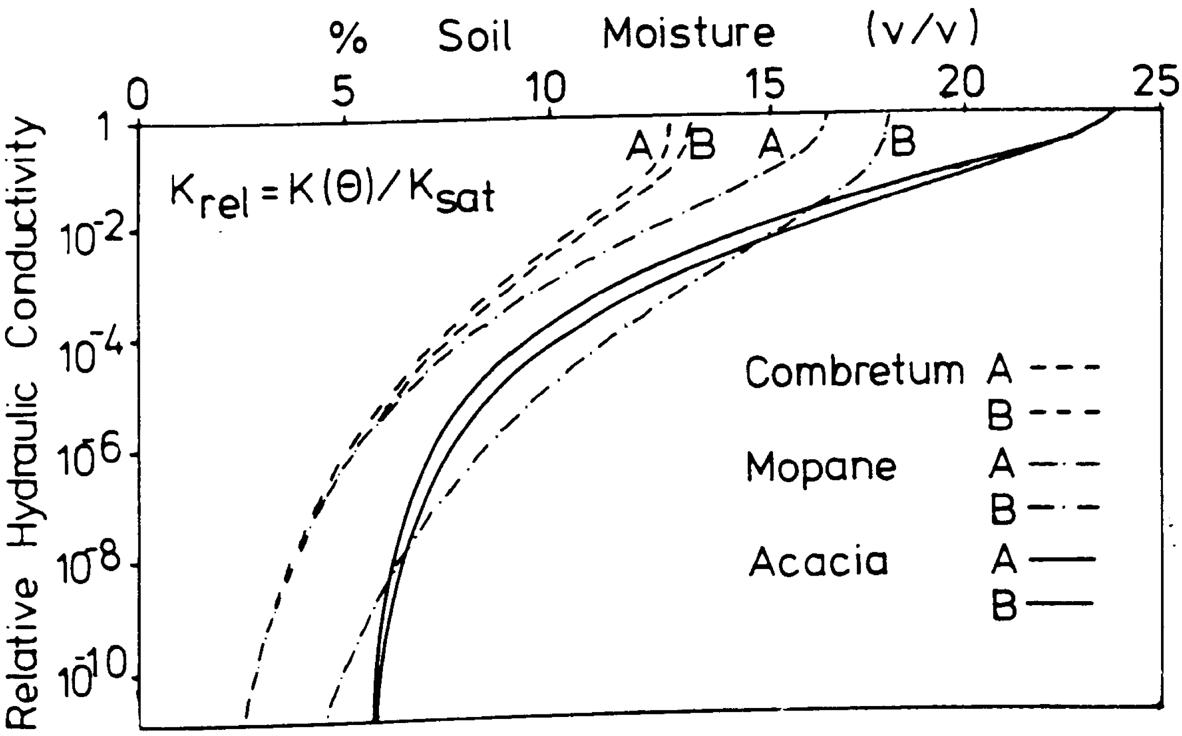

Figure 26. Calculated relative soil hydraulic conductivity

3.4.3 SOIL MOISTURE CONTENT

Soil moisture content was monitored routinely for each treatment at each site using an array of gypsum block sensors (Bourget, Elrick & Tanner 1958). Two types were used (for reasons of availability); Delmhorst blocks at the Mopane site and Beckman CEL-WFD blocks elsewhere. The arrays consisted of twelve blocks, equally divided between sub-canopy habitat and open areas, with two replications in each. Each replicate consisted of three blocks, buried at depths of 50 mm, 350 mm and 700 mm. These depths corresponded approximately with the soil surface layer, the transition from A to B horizons, and the B to C horizons.

A soil column approximately 1 m in diameter surrounding one of the sub-canopy replicates and one of the open replicates in the treatments destined to be bush-cleared were sterilised by the addition of 30 g of tebuthiuron ("Spike") to the soil surface. These columns functioned as controls, free of root water uptake. Soil water changes in these columns were therefore purely as a result of soil and atmospheric factors. Tebuthiuron has a soil half-life of about two years, and dosage was repeated annually at the beginning of the rainy season. No plants grew within the sterilised area and the moisture data from the columns suggest that no major recolonisation by roots from surrounding areas occurred. Tebuthiuron is inactivated by clays, and sterilisation of at least one of the Acacia site columns was incomplete.

Moisture could be lost from the root-free columns by evaporation or by vertical or lateral flow into the adjacent soil. The relative importance of lateral versus vertical flow was difficult to assess, but the persistence of moisture in the sterilised columns through the winter months (when the surrounding soil was dry) suggests that both were minor in comparison to evaporation.

Blocks were placed by augering separate holes for each, and tamping the block into position surrounded by sieved (<2 mm) soil of the same horizon. The lead wires were brought to a central metering point which was within 5 m of the placement. Blocks were placed at least three months before metering began to allow for equilibration.

Metering was via a circuit described by Goltz, Benoit & Schimmelpfenning (1981), modified by the addition of a selector switch to allow the entire array to be measured through a single connector. The accuracy of metering was greatly in excess of the accuracy of calibration of the blocks.

The blocks were individually calibrated against known soil water potentials in a pressure plate apparatus. Calibration was conducted at -30, -100, -200, -500, -1000 and -1500 kPa in sieved soil from the horizons in which the blocks were to be buried (Figure 27 on page 92), simultaneously with the determination of the soil characteristic curve. All soil moisture values were expressed on a volumetric basis. The calibrations

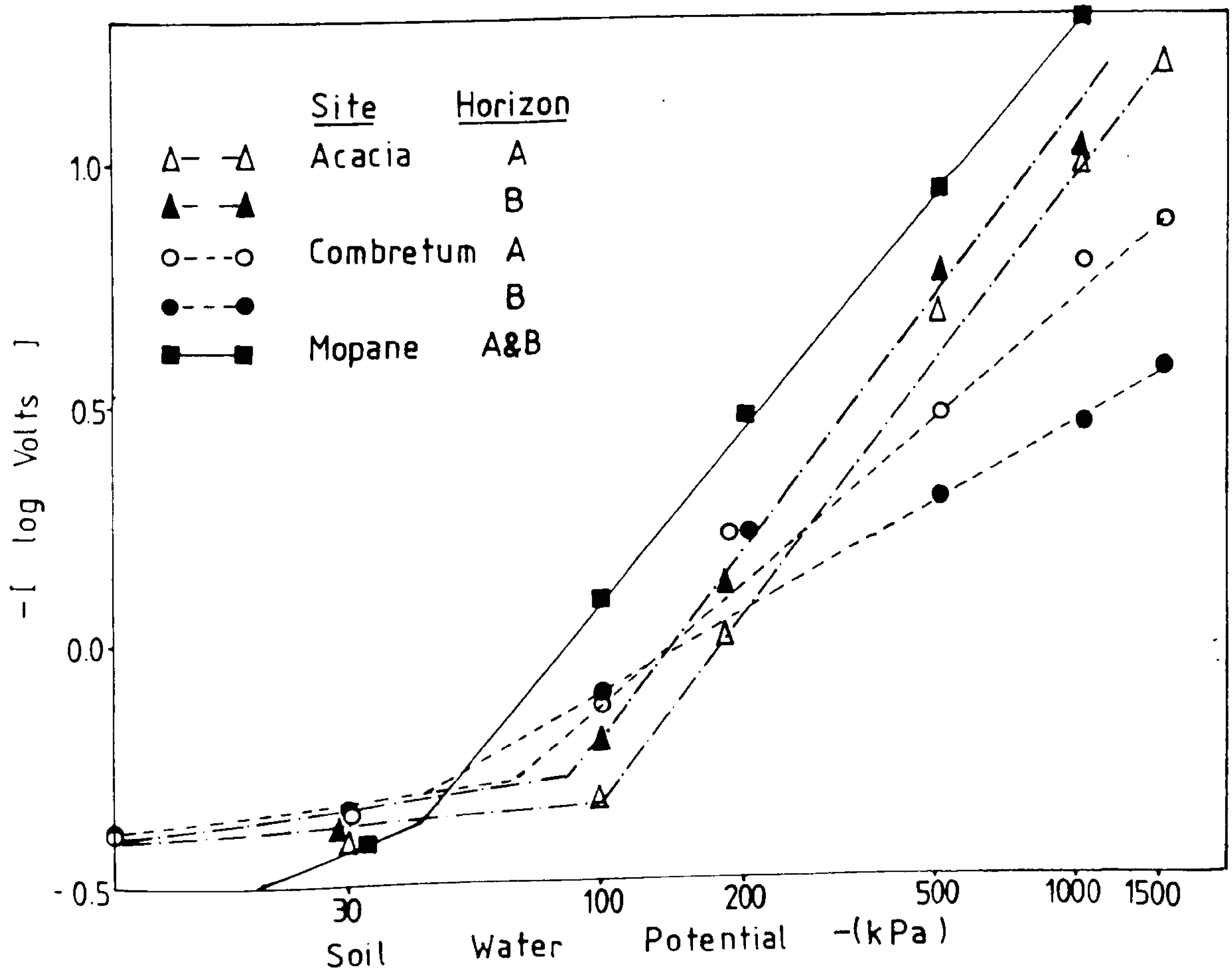

Figure 27. Mean calibration curves for gypsum moisture blocks on the pressure-plate apparatus.

were checked *in situ* by taking gravimetric moisture samples at the high and low extremes of the moisture range as indicated by the buried blocks. The laboratory and *in situ* calibrations were highly correlated, (Combretum site: $F=56.41$, $n=11$, $p<0.0001$; Mopane site: $F=44.07$, $n=9$, $p<0.0002$; Acacia site: $F=54.91$ $n=10$ $p<0.0001$) but the laboratory calibration overestimated the field moisture levels. This is due to the use of disturbed soils in the laboratory, as well as inherent inaccuracies in the pressure plate method. The *in situ* calibration was used in further calculations.

Soil temperatures were taken at each depth for the first season in order to correct for the temperature dependence of the blocks, but was found to fluctuate little on a daily basis, except at the surface. In relation to the accuracy which can reasonably be expected with the use of gypsum blocks the increase in precision did not justify the increase in effort required to make this correction.

A computer program was written to convert the meter readings (in volts) to soil water potential, via the calibration curves and then to soil moisture content via the characteristic curve. The soil moisture status data for the experiment are graphically summarised in Figure 28 on page 94, Figure 29 on page 95 and Figure 30 on page 96. In the graphics, the thickest lines represent periods of near-saturation (>-100 KPa), the medium lines moisture adequacy (100-500 KPa) and the thinnest lines partial stress (500-1500 KPa). Blank spaces occur where the soil water potential was below -1500 KPa. Blank spaces within the "wet" areas represent days on which no data were available; the water status is inferred from neighbouring records.

Soil moisture readings were taken daily after rainfall (when conditions permitted) until the soil reached wilting point (as determined from the vegetation condition) and thereafter every three days, or in times of prolonged drought, weekly. The sampling scheme was therefore neither random nor fully systematic, and the frequency of days on which the soil profile was recorded as having plant-available moisture ("wet days"; $\psi <$ -1500 kPa; Table 3.4) is positively biased relative to the true frequency. However, all the blocks were always measured on the same day, and the data can therefore be tested for differences in the duration of plant-available water between blocks using the χ^2 test of association. The unequal sample sizes are due to the use of half of the soil moisture blocks in the cleared treatments to monitor the root-free columns and to occasional electronic failures (hyenas and elephants were both intrigued by the exposed connector sockets). Where the term "overall" is used in the following discussions, it means that the treatment was regarded as being "wet" if plant available water was present at any depth at any one of the sensors (excluding those in the root-free columns, which constitute a treatment on their own).

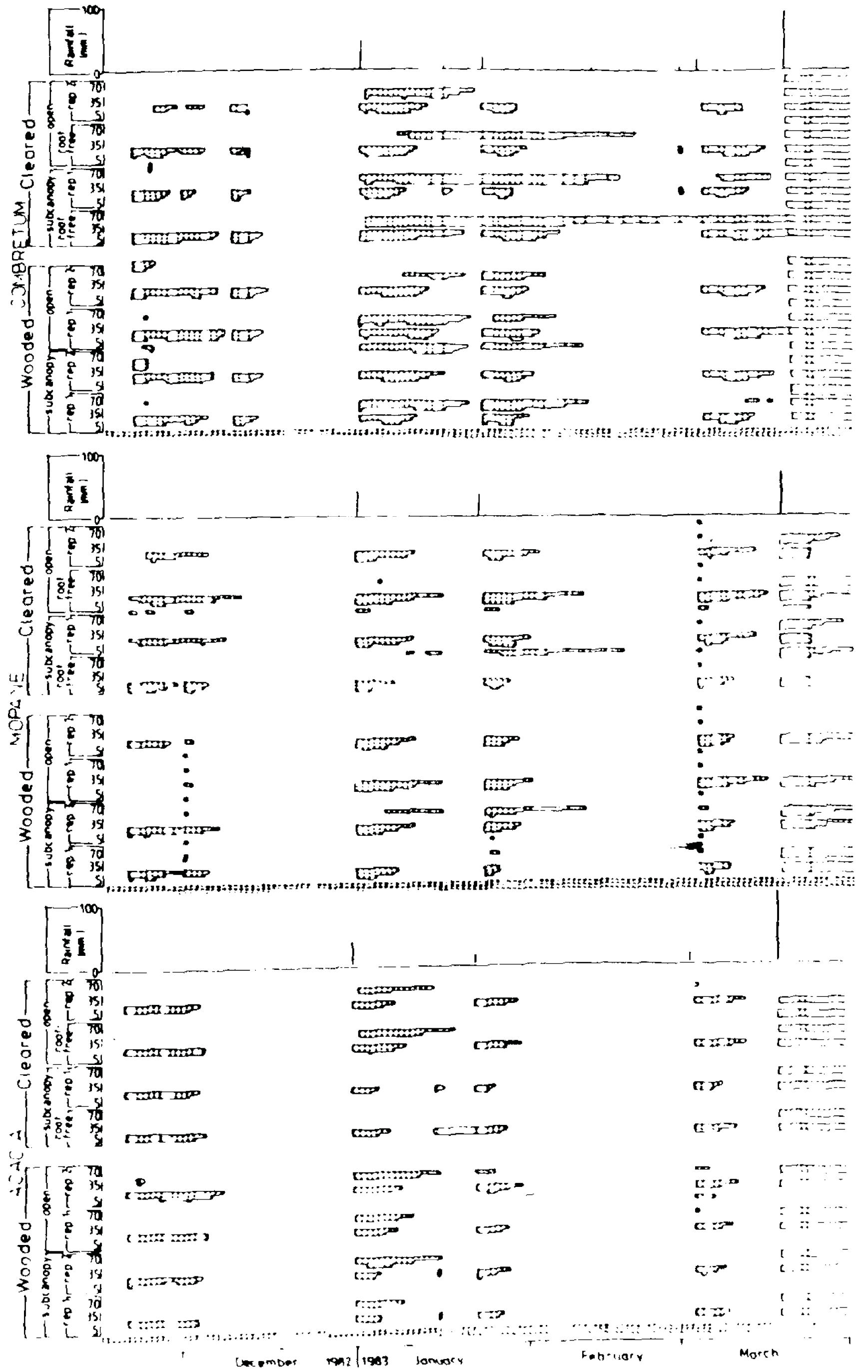

Figure 28. Soil moisture content during 1982/3 wet season: periods of plant-available moisture by site, treatment and depth. The thickness of the line indicates relative water availability.

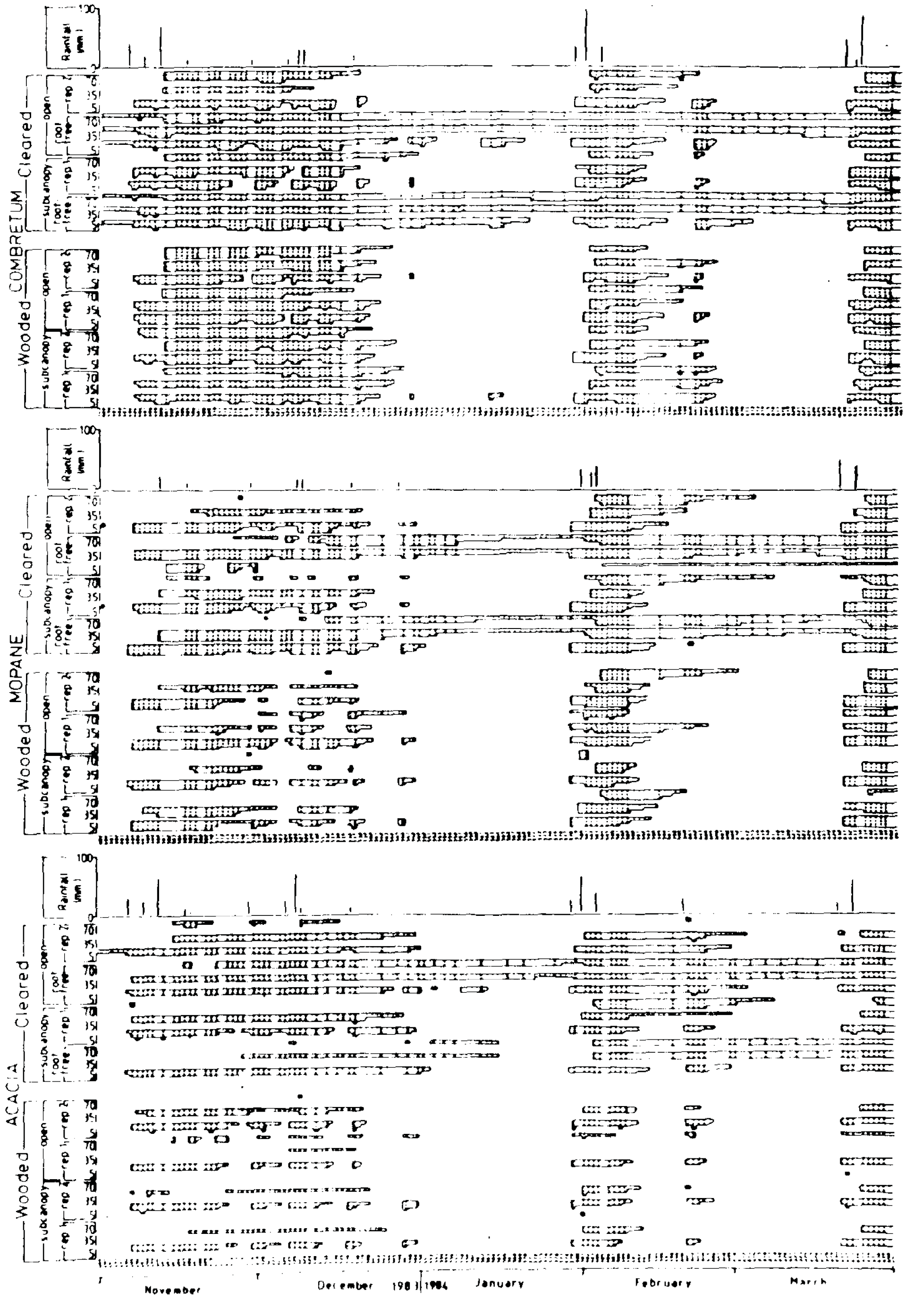

Figure 29. Soil moisture content during 1983/4 wet season: periods of plant-available moisture by site, treatment and depth. The thickness of the line indicates relative water availability.

Figure 30. Soil moisture content during 1984/5 wet season: periods of plant-available moisture by site, treatment and depth. The thickness of the line indicates relative water availability.

Table 3.4 The frequency of days without plant-available water in the soil profile ("dry") in treatments with and without woody plants.

Site & season	Depth (mm)	Wooded Dry	Wooded Wet	Cleared Dry	Cleared Wet	Frequency Dry Wooded	Frequency Dry Cleared	Chi square	Probability
Combretum 82/3	50	101	195	67	75	0.34	0.48	7.776	0.005 **
	350	199	97	85	59	0.67	0.59	2.848	0.092 *
	700	244	52	132	12	0.82	0.92	6.646	0.010
	all	13	61	8	66	0.18	0.11	1.387	0.239
83/4	50	97	231	53	109	0.30	0.33	0.504	0.478
	350	131	197	74	88	0.40	0.46	1.468	0.226
	700	145	183	70	92	0.44	0.43	0.044	0.834
	all	18	64	0	82	0.22	0.00	20.220	0.000 ***
84/5	50	116	320	63	153	0.27	0.29	0.476	0.515
	350	129	307	79	137	0.30	0.37	3.246	0.072 *
	700	146	290	61	155	0.33	0.28	1.834	0.176
	all	7	104	0	111	0.06	0.00	7.228	0.007 ***
Mopane 82/3	50	143	133	57	81	0.52	0.41	4.067	0.044 **
	350	241	35	130	8	0.87	0.94	4.684	0.030 **
	700	264	12	122	16	0.96	0.88	7.661	0.006 ***
	all	17	55	11	61	0.24	0.15	1.596	0.206
83/4	50	106	198	51	105	0.35	0.33	0.217	0.641
	350	149	155	75	81	0.49	0.48	0.036	0.849
	700	244	60	98	58	0.80	0.63	16.450	0.000 ***
	all	13	65	1	77	0.17	0.01	11.300	0.001 ***
85/6	50	77	339	22	184	0.19	0.11	6.312	0.012 **
	350	124	292	25	181	0.30	0.12	23.619	0.000 ***
	700	136	280	23	183	0.33	0.11	33.554	0.000 ***
	all	5	101	0	106	0.05	0.00	5.121	0.024 **
Acacia 82/3	50	157	135	85	63	0.54	0.57	0.533	0.465
	350	215	77	128	20	0.74	0.86	9.446	0.002 ***
	700	284	8	148	0	0.97	1.00	4.130	0.042 **
	all	25	49	27	47	0.34	0.36	0.119	0.731
83/4	50	116	212	38	128	0.35	0.23	7.994	0.005 ***
	350	190	138	57	109	0.58	0.34	24.533	0.000 ***
	750	290	38	131	35	0.88	0.79	7.897	0.005 ***
	all	19	65	0	84	0.23	0.00	21.423	0.000 ***
84/5	50	130	298	37	177	0.30	0.17	12.690	0.000 ***
	350	143	285	29	185	0.33	0.14	28.689	0.000 ***
	700	219	209	104	110	0.51	0.49	0.377	0.539 ***
	all	11	99	0	110	0.10	0.00	11.579	0.001 ***

*=90, **=95, ***=99 % level of confidence

3.4.3.1 Treatment effects

The problem of pseudoreplication must be borne in mind when interpreting the between-treatment statistical tests. In the Combretum and Mopane sites the cleared treatments tended to dry out more slowly than the wooded treatments in the early part of the season (when the grass biomass was low), but more rapidly late in the season. In the Acacia site drying was always fastest in the trees-and-grass treatment. Drying was to lower water potentials in the Combretum grassland than woodland site, but was comparable or inconsistent elsewhere.

There was no overall significant difference at the 90% confidence level between treatment plots in the frequency of wet days before the clearing treatment was imposed. This was true for all sites, although there were some significant differences at specific depths (Combretum: wooded>cleared at 50 & 700 mm; Mopane: cleared>wooded at 50 & 700mm but wooded>cleared at 350; Acacia: wooded>cleared at 350 & 700mm). These differences are attributed to the chance effects of spatial variability in soil moisture distribution. Although the number of samples was high due to replication in time, the spatial replication was low (only two per depth in the cleared treatments, and four per depth in the wooded treatments).

In all sites the cleared treatment was wetter overall than the wooded treatment in both post-clearing seasons. The strength of this effect, as indexed by the probability level, was in all cases greater in the first than the second post-clearing season, and was greatest in the Acacia site and least in the Mopane site.

In the Combretum site there were no statistically significant trends with depth, but the 700mm depth was wetter in the cleared treatment and the 50 and 350mm depths were drier in both post clearing seasons. In the Mopane site all depths were wetter in the cleared treatment, although only the 700mm depth was significantly so during the first season. In the second season all depths were significantly wetter in cleared treatment, with the effect being strongest at the 700mm depth. In the Acacia site all depths were significantly wetter in the cleared site during both seasons except for the 700mm depth in the second season, where the difference was not statistically significant. The treatment effect was strongest at the 350mm depth.

It is therefore concluded that bush clearing results in an immediate increase in the duration of plant-available water in the soil profile. These results agree with those of Strang (1969a) and Pratchett (1978). This effect may gradually be lost as the grass biomass increases and therefore increases the moisture demand, but will probably persist if rain falls at times of the year when grasses are physiologically inactive, or in amounts large enough to penetrate beyond the zone where most grass roots are found. The depth at which the effect is most strongly expressed increases with decreasing water-holding capacity, and the strength of the effect (in this study) is related to soil texture rather than to the tree leaf biomass before clearing.

3.4.3.2 Root-free columns

The persistence of moisture in the deeper horizons of the root-free columns once wetted is apparent for all sites, and especially so in the Combretum site where evaporation is low due to the sandiness of the soil. This shows that the permeability of the underlying strata (vertical flow) and the unsaturated hydraulic conductivity (lateral flow) are both small. The consequences of an excess of moisture in the profile are therefore likely to be lateral saturated flow above the lithic contact. Water penetration to the deeper horizons occurs most readily in the Combretum site and least frequently in the Acacia site, as would be expected from the water-holding capacity and hydraulic conductivity data. Evaporation was effective to greater depths in the Acacia and Mopane sites due to the increased depth of the capillary fringe with decreasing soil pore size.

Table 3.5 Frequency of days with no plant-available water in the soil profile ("dry") in sub-canopy and open habitats of wooded grasslands.

Site & season	Depth (mm)	Sub-canopy Dry	Sub-canopy Wet	Open Dry	Open Wet	Frequency Dry Sub	Frequency Dry Open	Chi square	Probability
Combretum	50	47	101	54	94	0.32	0.36	0.736	0.391
82/3	350	96	52	103	45	0.65	0.70	0.751	0.386
	700	135	13	109	39	0.91	0.74	15.770	0.000 ***
83/4	50	50	114	47	117	0.30	0.29	0.132	0.717
	350	68	96	63	101	0.41	0.38	0.318	0.573
	700	77	87	68	96	0.47	0.41	1.001	0.317
84/5	50	68	150	48	170	0.31	0.22	4.698	0.030 **
	350	78	140	51	167	0.36	0.23	8.026	0.005 ***
	700	84	134	62	156	0.39	0.28	4.984	0.026 **
Mopane	50	71	67	72	66	0.51	0.53	0.015	0.904
82/3	350	135	3	106	32	0.98	0.77	25.518	0.000 ***
	700	133	5	131	7	0.96	0.95	0.348	0.555
83/4	50	50	102	56	96	0.33	0.37	0.521	0.470
	350	67	85	82	70	0.44	0.54	2.962	0.085
	700	106	46	138	14	0.70	0.91	21.263	0.000 ***
84/5	50	32	176	45	163	0.15	0.22	2.693	0.101
	350	64	144	60	148	0.31	0.29	0.184	0.668
	700	58	150	78	130	0.28	0.38	4.370	0.037 **
Acacia	50	70	76	87	59	0.48	0.60	3.982	0.046 **
82/3	350	102	44	113	33	0.70	0.77	2.134	0.144
	700	140	6	144	2	0.96	0.99	2.056	0.152
83/4	50	59	105	57	107	0.36	0.35	0.053	0.817
	350	103	61	87	77	0.63	0.53	3.202	0.074 *
	700	128	36	162	2	0.78	0.99	34.469	0.000 ***
84/5	50	55	159	75	139	0.26	0.35	4.419	0.036 **
	350	75	139	68	146	0.35	0.32	0.515	0.473
	700	113	101	106	108	0.53	0.50	0.458	0.498

*=90, **=95, ***=99 % level of confidence

3.4.3.3 Tree canopy effects

The hydrology of the microhabitat immediately below the canopy of a large tree differs from that between tree canopies due to differences in both water supply and water demand. It is impossible to say *a priori* which habitat will be wetter since it is the resultant of several conflicting processes; increased stemflow, herbaceous biomass and infiltration but decreased precipitation and radiant energy.

A comparison of the frequency of "dry" sample days between sub-canopy and between-canopy habitats is given in Table 3.5. In the Combretum site the whole profile tended to be wetter between than beneath canopies, although the difference was only significant in the wet 1984/5 season, and at 700mm in the dry 1982/3 season. This result could reflect the dominant effect of interception losses in this site where infiltration rates are always high.

In the Mopane site, where the difference between habitats was significant, the open sites were drier at the 700 mm depth (350 mm in the 1982/3 season) indicating deeper penetration of moisture beneath than between canopies. This is in agreement with the findings of Pressland (1973), and may reflect the relatively high contribution by stemflow in this site.

In the Acacia site the between-canopy habitat was also drier than the sub-canopy habitat whenever the difference was significant, although the depth at which the effect occurred varied between seasons. In both the wettest and driest seasons the biggest difference was in the surface soil layers, while in the 1983/4 season it occurred at 700 mm. Overall there was a non-significant trend for the between-canopy habitat to be drier in dry seasons and wetter in wet seasons than the sub-canopy habitat. These differences could be due to the marked changes in grass biomass and species composition that occurred at this site between dry and wet years. The difference was retained after clearing.

3.5 EVAPOTRANSPIRATION

3.5.1 PAN EVAPORATION

The annual course of Class A pan evaporation, an approximate index of atmospheric evaporative demand, is illustrated in Figure 31 on page 102. It is well fitted by a cosine function ($F=262.8$, $n=182$, $p<0.0001$),

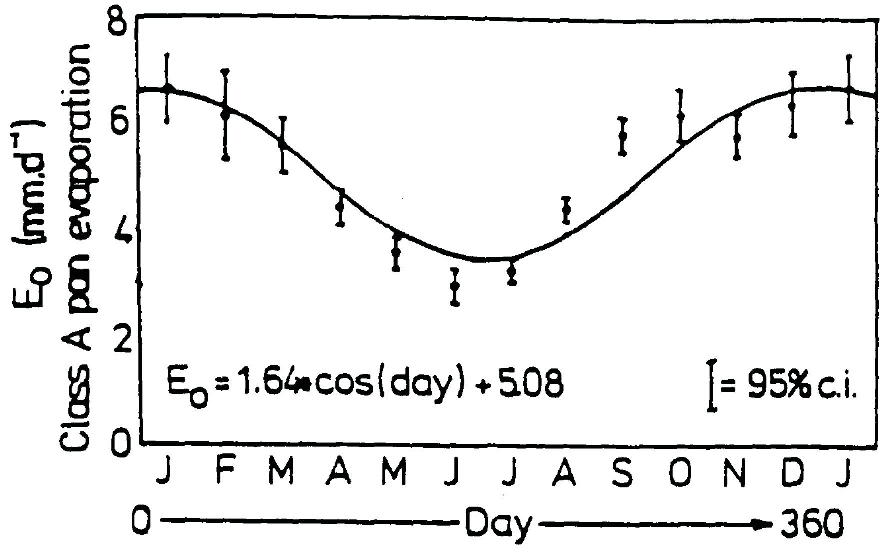

Figure 31. Annual course of Class A pan evaporation: based on 14 years data from Skukuza

suggesting that potential evapotranspiration is largely controlled in this region by radiant energy supply. The depression in November is probably due to the cloudiness and high humidity associated with that month.

3.5.2 EVAPORATION FROM THE SOIL SURFACE

The theory governing evaporation from a bare soil surface is detailed by Philip (1957) and Black, Gardner and Thurtell (1969). The general pattern is an initial phase of rapid, almost constant rate evaporation, followed by a phase of declining rates where the cumulative evaporation is proportional to the moisture content of the upper profile. The transition between the two phases can be quite sharp. In broad terms, the initial rates are limited by atmospheric factors (the evaporative potential and energy flux) while soil factors (the thermal and hydraulic conductivity) are limiting during the falling-rate phase.

Rates of evaporation from the soil were determined at each site by the repeated weighing of soil-filled lysimeters (Figure 32 on page 104). The lysimeters were packed with soil from the A horizon to a density approximating the *in situ* soil bulk density. The lysimeters were cylindrical with a perforated base draining into a container for collecting moisture percolating through the entire column. They were embedded in the soil inside closely fitting housings so that the top of the soil column was level with the soil surface. The housing projected 10 mm above the soil to prevent runoff from swamping the lysimeter.

During the 1982/3 season, the lysimeters were constructed of PVC pipe with an internal diameter of 103 mm enclosing a soil column 150 mm long. Weighing was on an Ohaus triple beam balance to a theoretical resolution of 0.1 g (equivalent to 0.01 mm of water). During the 1983/4 season the lysimeters were constructed of tin plate (modified 5 *l* double-container paint tins) with a soil column diameter of 170 mm and length of 240 mm. Weighing was on a Ktron electronic balance via a mass dividing beam to a theoretical resolution of 0.1 g (0.02 mm of water). The theoretical resolutions were not obtainable under windy field conditions, and readings were taken to the nearest 0.2 mm of water.

The lysimeters were weighed on the same occasions as soil moisture was metered. When water had collected in the bottom container, the lysimeters were weighed before and after emptying the accumulated liquid.

Four lysimeters were installed per study site, in the uncleared treatment. Two were placed under tree canopies and two away from tree canopies. The soil columns were kept free of plant growth. Examples of lysimeter drying curves are shown in Figure 33 on page 105
and evaporation values during the constant-rate phase are given in Table 3.6. Homogeneity of slope tests show all the rates to be significantly different from one another at the 95% confidence level, indicating a high spatial variability. The difference between samples was in most cases greater than the difference between treatments, but evaporation

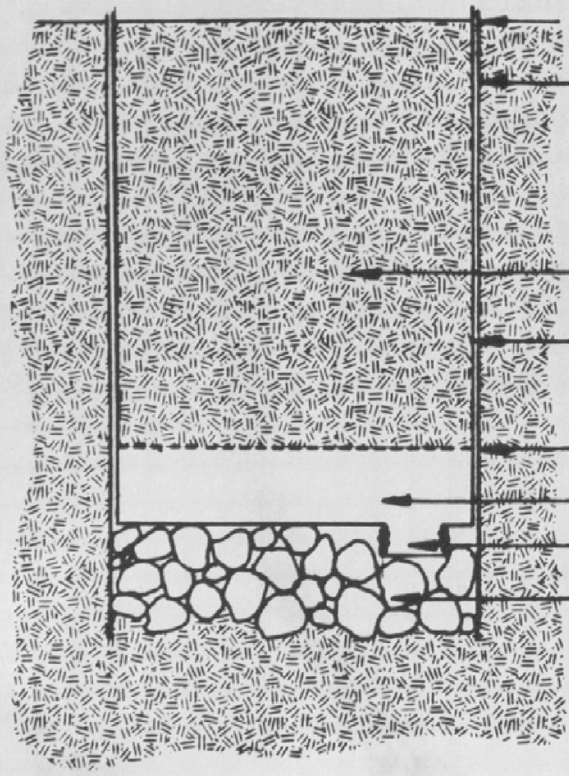

Figure 32. Lysimeter design

in the open was usually slower than in the sub-canopy habitat. Evaporation during the constant rate phase, which contributed about 75% of the water lost by evaporation, was highest at the Mopane site and lowest at the Combretum site, again illustrating the fallacy of assuming that all soil physical parameters mirror the clay-content continuum.

Evaporation from the soil surface is a major component of the hydrological cycle in semi-arid regions (Whitmore 1971), with a magnitude of a similar order to that of transpiration. The finding that it was inversely related to the level of radiant energy received at the soil surface, in apparent contradiction to theory (Nakano, Cho & Hillel 1983), was therefore investigated further.

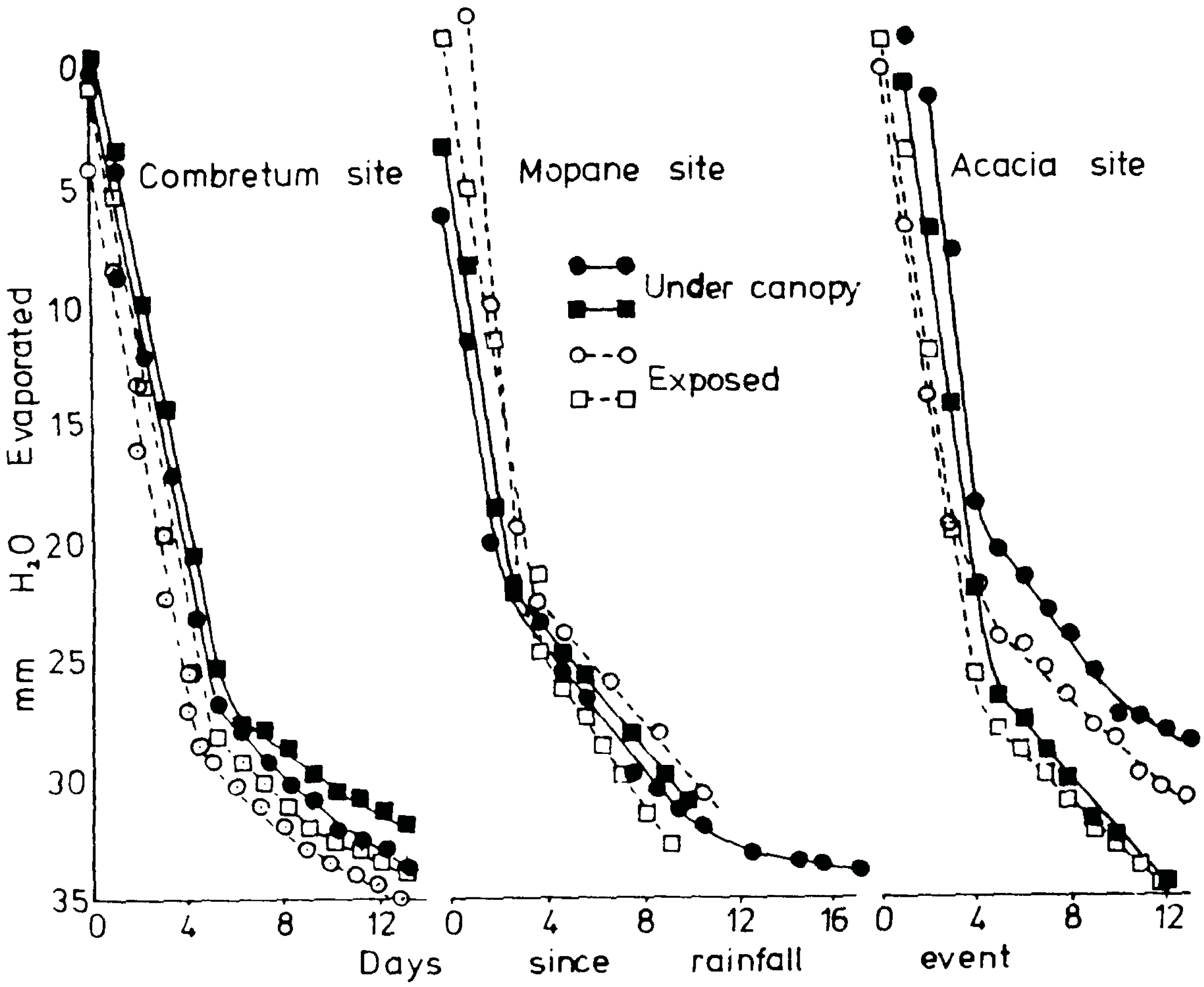

Figure 33. Lysimeter drying curves: O=Rep 1, II=Rep 2.

The lysimeters, still filled with soil from the three sites, were installed at a central location and shaded 100, 70, 50 and 0% with commercial shade cloth. The lysimeters were wetted with rainwater and the evaporation rates were monitored daily through four drying cycles, the shading level being rotated for each cycle.

The results of this experiment are illustrated in Figure 34 on page 107. Shading only slightly reduced the evaporation rate, and the relationship between irradiance and evaporation is complex. Since all the field lysimeters were shaded to some degree at different times of the day, and were within the grass canopy boundary layer, it is not possible to make a direct comparison between the field data and the shading experiment. It is suggested that the evaporation rate under conditions of high atmospheric demand is limited mainly by the ability of the soil to transport moisture upwards to the soil surface, even during the initial drying phase. Under high irradiance, high evaporation conditions a barrier of dry soil with a consequently low hydraulic conductivity forms at the soil surface, which retards further evaporation. As a consequence, shading has only a slight effect on evaporation from the soil surface.

When the atmosphere is hot and dry, as it is most of the time in the semi-arid savannas, a large component of the energy required to drive evaporation from the soil (or plant) surface is provided by sensible heat, which can be advected from neighbouring unshaded patches. Harrison (in prep) found that sensible heat contributed a large proportion of the sub-canopy thermal balance in the savanna at Nylsvley. Therefore the

Table 3.6 Evaporation rates from a bare soil surface during the constant-rate phase (rates > 1 $mm.d^{-1}$).

Site	Sub-habitat		mean	s.d.	n	Habitat mean	Pooled mean
				$mm.d^{-1}$			
Combretum	Open	1	2.4	2.0	21		
		2	2.8	2.0	22	2.60	
	Subcanopy	3	2.7	2.1	23		
		4	3.0	2.4	22	2.85	2.73
Mopane	Open	1	3.1	2.2	16		
		2	2.8	2.2	21	2.95	
	Subcanopy	3	4.3	3.5	19		
		4	4.0	3.6	18	4.15	3.55
Acacia	Open	1	2.5	2.2	33		
		2	3.5	3.1	35	3.00	
	Subcanopy	3	2.9	2.4	35		
		4	2.9	2.3	37	2.90	2.95

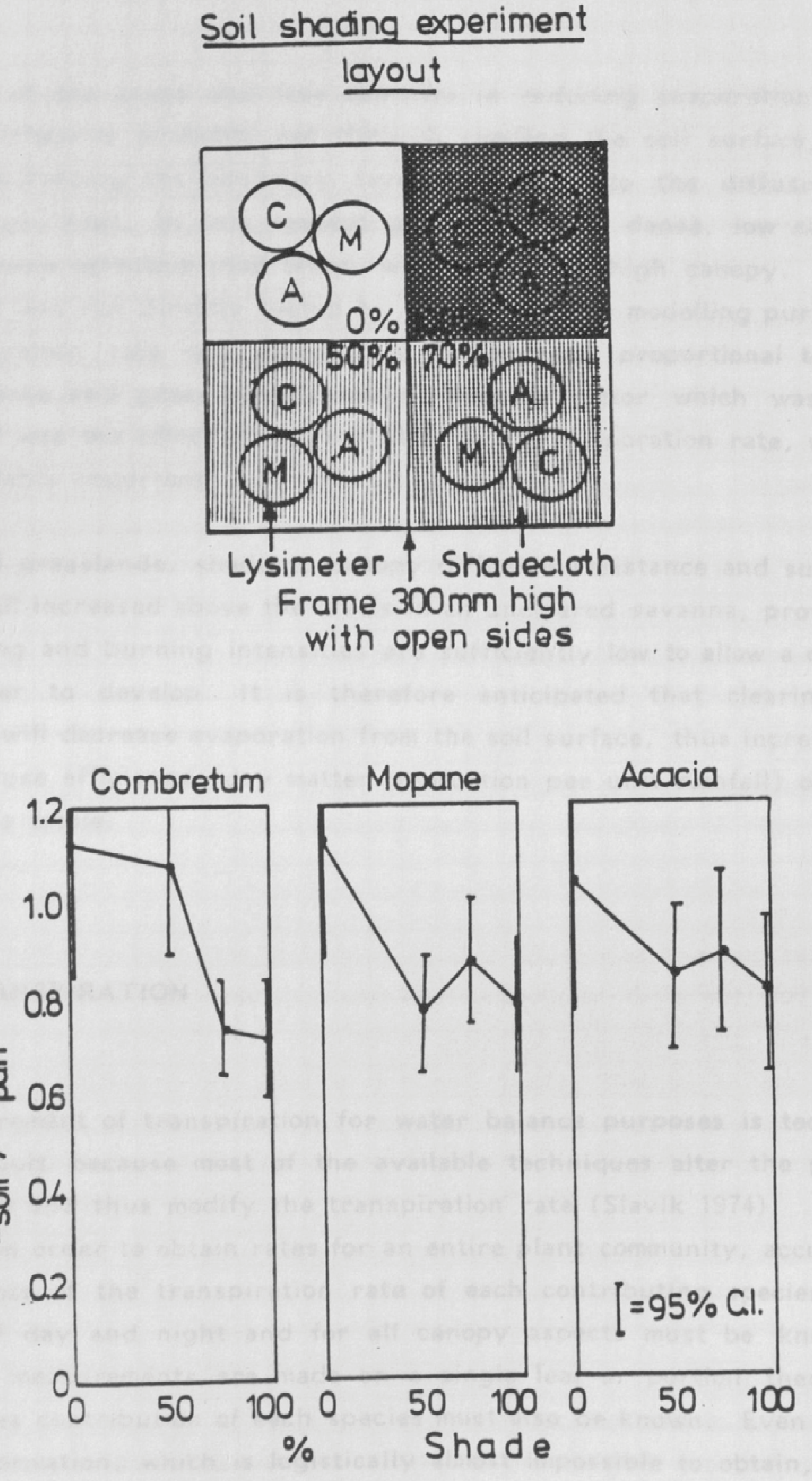

Figure 34. Influence of shade intensity on evaporation from the soil: bars indicate 95% confidence intervals.